

Design, Synthesis, Enzyme-Inhibitory Activity, and Effect on Human Cancer Cells of a Novel Series of Jumonji Domain-Containing Protein 2 Histone Demethylase Inhibitors

Shohei Hamada,[†] Takayoshi Suzuki,^{*,†,‡} Koshiki Mino,[§] Koichi Koseki,[§] Felix Oehme,^{||} Ingo Flamme,^{||} Hiroki Ozasa,[†] Yukihiro Itoh,[†] Daisuke Ogasawara,[†] Haruka Komarashi,[§] Aiko Kato,[§] Hiroki Tsumoto,[†] Hidehiko Nakagawa,[†] Makoto Hasegawa,[§] Ryuzo Sasaki,[⊥] Tamio Mizukami,^{*,§} and Naoki Miyata^{*,†}

[†]Graduate School of Pharmaceutical Sciences, Nagoya City University, 3-1 Tanabe-dori, Mizuho-ku, Nagoya, Aichi 467-8603, Japan, [‡]PRESTO, Japan Science and Technology Agency (JST), 4-1-8 Honcho Kawaguchi, Saitama 332-0012, Japan, [§]Graduate School of Bio-Science, Nagahama Institute of Bio-Science and Technology, 1266 Tamura-cho, Nagahama, Shiga 526-0829, Japan, ^{||}Bayer Schering Pharma AG, Institute for Cardiovascular Research, Aprather Weg 18a, D-42096 Wuppertal, Germany, and [⊥]Frontier Pharma Inc., 1281-8 Tamura-cho, Nagahama, Shiga 526-0829, Japan

Received March 23, 2010

Selective inhibitors of Jumonji domain-containing protein (JMJD) histone demethylases are candidate anticancer agents as well as potential tools for elucidating the biological functions of JMJDs. On the basis of the crystal structure of JMJD2A and a homology model of JMJD2C, we designed and prepared a series of hydroxamate analogues bearing a tertiary amine. Enzyme assays using JMJD2C, JMJD2A, and prolyl hydroxylases revealed that hydroxamate analogue **8** is a potent and selective JMJD2 inhibitor, showing 500-fold greater JMJD2C-inhibitory activity and more than 9100-fold greater JMJD2C-selectivity compared with the lead compound *N*-oxalylglycine **2**. Compounds **17** and **18**, prodrugs of compound **8**, each showed synergistic growth inhibition of cancer cells in combination with an inhibitor of lysine-specific demethylase 1 (LSD1). These findings suggest that combination treatment with JMJD2 inhibitors and LSD1 inhibitors may represent a novel strategy for anticancer chemotherapy.

Introduction

Reversible methylation of histone lysine residues, which is tightly controlled by histone methyltransferases and histone demethylases, is responsible for the regulation of epigenetic gene expression.¹ To date, two classes of histone lysine demethylases have been identified. One class includes lysine-specific demethylase 1 (LSD1^a) and LSD2, which are flavin-dependent amine oxidase domain-containing enzymes.² The other class comprises the recently discovered Jumonji domain-containing protein (JMJD) histone demethylases.^{1c,3} JMJDs have been reported to remove the methyl groups from methylated lysines of histone H3 through Fe(II)/ α -ketoglutarate-dependent enzymatic oxidation.^{1c,3,4}

While there is only limited information about the biological functions of JMJDs, it has been reported that JMJDs are associated with cancer.^{1c} For example, overexpression of JMJD2C, a member of the JMJD histone demethylase family, increases the expression of Mdm2 oncogene in a manner dependent on JMJD2C's demethylase activity, leading to a decrease of p53 tumor suppressor gene product in the cells.⁵ Furthermore, the outcome of RNAi-mediated knockdown of JMJD2C suggested that this enzyme is associated with cell growth of esophageal squamous cancer,⁴ prostate cancer,⁶ and breast cancer.⁷

Therefore, selective inhibitors of JMJDs, including JMJD2C, are potential tools to study the functions of these enzymes and are also candidate anticancer agents having few side effects.

Several types of JMJD inhibitors have been identified so far. Succinic acid has been suggested to inhibit JMJD2D by product inhibition.⁸ 2,4-Pyridinedicarboxylic acid (PCA, **1**) (Chart 1), which inhibits other Fe(II)/ α -ketoglutarate-dependent oxygenases, was also reported to be a potent inhibitor of JMJD2A and 2E⁹ but has not been tested in a cellular assay. *N*-Oxalylglycine (NOG, **2**), the amide analogue of α -ketoglutarate, and its derivatives have been reported to inhibit JMJD2 proteins in vitro.^{4,10,11} In particular, *N*-oxalyl-D-tyrosine derivative **3** showed selective inhibition of JMJD2 over prolyl hydroxylase domain-containing protein 2 (PHD2), another Fe(II)/ α -ketoglutarate-dependent enzyme that hydroxylates hypoxia-inducible factor (HIF), although again, a cellular assay was not employed.¹¹ In addition, a disulfiram analogue has been shown to inhibit JMJD2A by removing a Zn ion from the Zn-binding site.¹² To our knowledge, there has been no report describing cell-active JMJD-selective inhibitors. Therefore, we initiated a search for novel JMJD inhibitors, with the goal of drug discovery, as well as finding new tools for biological research. In the present report, we describe the design, synthesis, enzyme-inhibitory activity, and cellular activity of a novel series of JMJD2 inhibitors.

Chemistry

The routes used for the synthesis of compounds **4–18**, which were prepared for this study, are shown in Schemes 1–7. Scheme 1 shows the preparation of acetohydroxamate **4**. Michael addition of *O*-benzylhydroxylamine to *tert*-butyl acrylate **19** afforded amine **20**. Amine **20** was treated with acetyl

*To whom correspondence should be addressed. Phone and fax: +81-52-836-3407. E-mail: suzuki@phar.nagoya-cu.ac.jp (T.S.); mizukami@nagahama-i-bio.ac.jp (T.M.); miyata-n@phar.nagoya-cu.ac.jp (N.M.).

^aAbbreviations: JMJD, Jumonji domain-containing protein; LSD, lysine-specific demethylase; PCA, pyridinedicarboxylic acid; NOG, *N*-oxalylglycine; PHD, prolyl hydroxylase domain-containing protein; HIF, hypoxia-inducible factor; DMPCA, dimethylester prodrug of PCA; FDH, formaldehyde dehydrogenase.

chloride to yield *O*-benzylacetohydroxamate **21**. The benzyl group of compound **21** was removed by hydrogenation to give hydroxamate **22**. Removal of the *tert*-butyl group of **22** using TFA afforded the desired compound **4**.

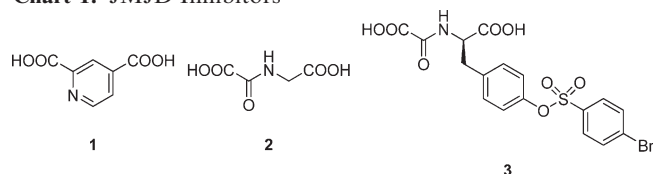
The routes for the synthesis of compounds **5–11** are illustrated in Scheme 2. Condensation of amine **20** with an appropriate acid chloride gave amides **23–29**. Bromides **23–29** were reacted with dimethylamine to give *tert*-amines **30–36**. Removal of the benzyl group of compounds **30–36** afforded hydroxamates **37–43**. Treatment of *tert*-butyl esters **37–43** with hydrochloric acid yielded compounds **5–11**.

The preparation of alkyl compound **12** is shown in Scheme 3. Acid chloride of **44** was reacted with amine **20** to give corresponding amide **45**. Deprotection of the benzyl group of **45** by hydrogenation and subsequent removal of the *tert*-butyl group of **46** afforded compound **12**.

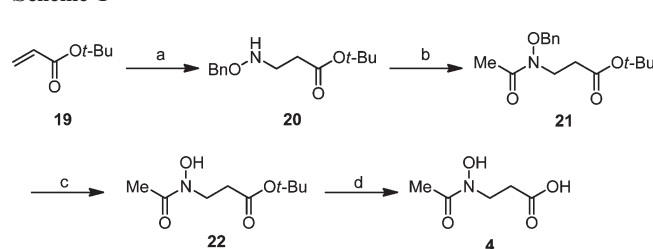
Scheme 4 shows the preparation of retro-hydroxamate **13**. Carboxylic acid **47** was treated with *O*-benzylhydroxylamine in the presence of EDCI and HOBt to give amide **48**. Treatment of amide **48** with 1,8-dibromooctane in the presence of sodium hydride yielded the *N*-alkylated compound **49**. Compound **13** was prepared from bromide **49** by using the procedure described for the synthesis of **5–11**.

Scheme 5 illustrates the synthesis of compound **14**. Reaction of compound **26** with *n*-butylmethylamine gave compound **52**. Compound **52** was converted to compound **14** using the procedure described for the synthesis of **5–11**.

Chart 1. JMJD Inhibitors

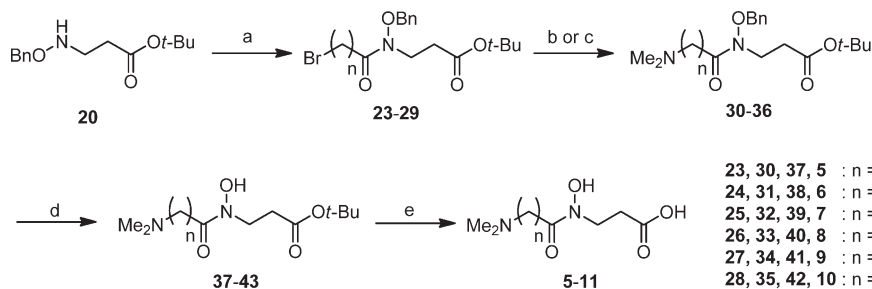


Scheme 1^a



^a Reagents and conditions: (a) *O*-benzylhydroxylamine, Et₃N, 1,4-dioxane, reflux, 44%; (b) AcCl, Et₃N, DMAP, CH₂Cl₂, room temp, 90%; (c) H₂, Pd/C, AcOEt, room temp, 80%; (d) TFA, CH₂Cl₂, room temp, 76%.

Scheme 2^a

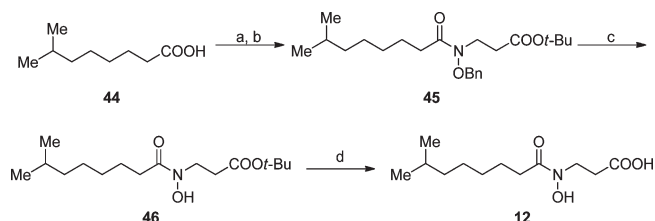


^a Reagents and conditions: (a) Br(CH₂)_nCOCl, Et₃N, DMAP, CH₂Cl₂, room temp, 32–79%; (b) Me₂NH, Et₃N, 1,4-dioxane, reflux, 49% for **30**; (c) Me₂NH, MeCN, reflux, 38–83% for **31–36**; (d) H₂, Pd/C, AcOEt, room temp, 34–77%; (e) HCl, 1,4-dioxane, CH₂Cl₂, room temp, 8–100%.

The synthesis of compounds **15** and **16** is outlined in Scheme 6. Compound **26** was reacted with benzylmethylamine to yield compound **54**. Catalytic reduction of *O*-benzyl compound **54** gave a mixture of *N*-benzyl compound **55** and *N*-debenzylated compound **56**. Treatment of the mixture of **55** and **56** with hydrochloric acid, followed by preparative HPLC separation, gave compounds **15** and **16**.

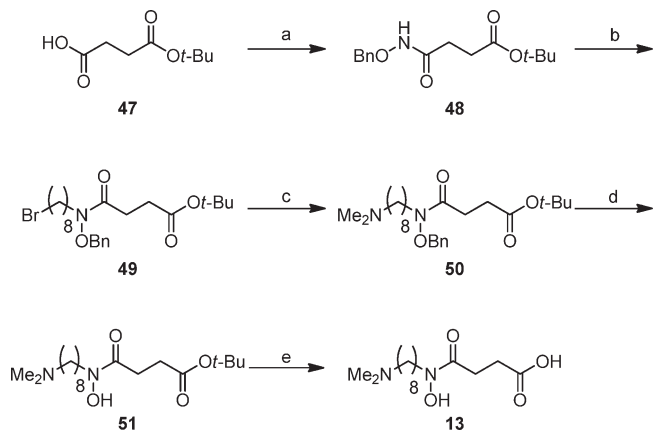
Scheme 7 shows the synthesis of compounds **17** and **18**. Michael addition of *O*-benzylhydroxylamine to methyl acrylate **57** afforded amine **58**. Amine **58** was treated with 9-bromononanoyl chloride to yield compound **59**. Compound **59** was reacted with dimethylamine to give **60**. Removal of the benzyl group of compound **60** gave compound **17**. *O*-Acetylation of compound **17** afforded compound **18**.

Scheme 3^a



^a Reagents and conditions: (a) (COCl)₂, DMF, CH₂Cl₂, room temp; (b) **20**, Et₃N, DMAP, CH₂Cl₂, room temp, 63% (two steps); (c) H₂, Pd/C, AcOEt, room temp, 82%; (d) HCl, 1,4-dioxane, CH₂Cl₂, room temp, 46%.

Scheme 4^a



^a Reagents and conditions: (a) *O*-benzylhydroxylamine, EDCI, HOBt·H₂O, DMF, room temp, 39%; (b) NaH, 1,8-dibromooctane, DMF, 50 °C, 42%; (c) Me₂NH, MeCN, reflux, 38%; (d) H₂, Pd/C, AcOEt, room temp, 100%; (e) HCl, 1,4-dioxane, CH₂Cl₂, room temp, 37%.

23, 30, 37, 5 : n = 5
24, 31, 38, 6 : n = 6
25, 32, 39, 7 : n = 7
26, 33, 40, 8 : n = 8
27, 34, 41, 9 : n = 9
28, 35, 42, 10 : n = 10
29, 36, 43, 11 : n = 11

Results and Discussion

Enzyme Assays. In 2007, Ng et al. reported the X-ray crystal structure of JMJD2A complexed with NOG (**2**) and histone trimethylated lysine peptide (PDB ID 2OQ6).¹³ The oxalyl group of NOG (**2**) interacts with Fe(II), and the other carboxyl group forms a hydrogen bond with Tyr 132 in the active center of the enzyme. In addition, the trimethylamino group of histone trimethylated lysine peptide is surrounded by Gly 170, Tyr 177, Glu 190, and Ser 288. The distances between the oxygens of the amino acid residues and the methyl groups of the histone trimethylated lysine peptide are less than 3.7 Å, being consistent with CH \cdots O hydrogen bonding. Because a CH group adjacent to an ammonium cation was calculated to form a stable hydrogen bond with amide oxygen, even in water,¹⁴ it is assumed that JMJDs, including JMJD2, recognize the methylated lysine substrate via CH \cdots O hydrogen bonds.

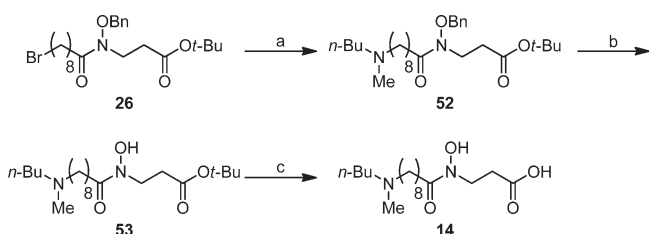
On the basis of this structure, we designed and prepared potential inhibitors of JMJD2, which has been reported to be

implicated in cancer cell growth, and tested them in two in vitro assay (Table 1 and Supporting Information Figure S1).^{4–7} In in vitro JMJD2C assay, PCA (**1**) and NOG (**2**) inhibited JMJD2C, with IC₅₀ values of 9.4 and 500 μM, respectively. PCA (**1**) and NOG (**2**) also inhibited JMJD2A with low IC₅₀ values (4.2 and 250 μM, respectively) as compared with JMJD2C. Initially, we designed compound **4** in which the oxalyl moiety of α-ketoglutarate is replaced with hydroxamate, a powerful metal ion chelator. As expected, a pronounced JMJD2-inhibitory effect (IC₅₀ = 34 μM for JMJD2C; 14 μM for JMJD2A) was observed with hydroxamate **4**, which was more than 10 times more active than NOG (**2**) and approximately 4-fold less potent than PCA (**1**).

Encouraged by this finding, we next designed compounds **5–11**, in which compound **4** is connected with a dimethylamino group through a linker. The homology model of JMJD2C, which was developed based on the crystal structure of JMJD2A, also suggested that the CH groups of the methylated lysine substrate form CH \cdots O hydrogen bonds with the amino acid residues of JMJD2C (Figure 1). We therefore anticipated that the methyl groups of the protonated dimethylamino moiety would form CH \cdots O hydrogen bonds with the carbonyl of Gly 172, the hydroxyl group of Tyr 179, the carboxylate of Glu 192, and the hydroxyl group of Ser 290 in the active site of JMJD2C, which might lead to potent inhibition of JMJD2C. Furthermore, compounds **5–11** were expected to inhibit JMJD2 more selectively over PHDs than compounds **1**, **2**, and **4**, because the X-ray crystal structure of PHD2 complexed with NOG (**2**) and HIF1α (PDB ID 3HQJ) has shown that there are hydrophobic (Val 241, Trp 258, and Trp 359) and positively charged amino acid residues (Arg 252 and Arg 322) around the active site (Supporting Information Figure S2),¹⁵ which would repulsively interact with the positively charged protonated dimethylamino group of compounds **5–11**. Compounds **5–11**, with various linker lengths, were synthesized, and their inhibitory activities toward JMJD2 were evaluated. As shown in Table 1, most of the dimethylamine-linked series exhibited potencies greater than those of the parent compound **4**. In particular, compounds **7–9**, with seven to nine methylene chains, showed IC₅₀ values in the low micromolar range against JMJD2C (1.0–1.6 μM). To examine the importance of the amino group of this series of compounds, we prepared compound **12**, in which the nitrogen of compound **5** is replaced with a carbon, and evaluated its JMJD2-inhibitory activity. As a result, compound **12** was much less potent than the parent compound **5**. The reason for the weak activity of compound **12** is unclear, but it is assumable that it is due to the loss of CH \cdots O hydrogen bonds between the inhibitor and the protein.

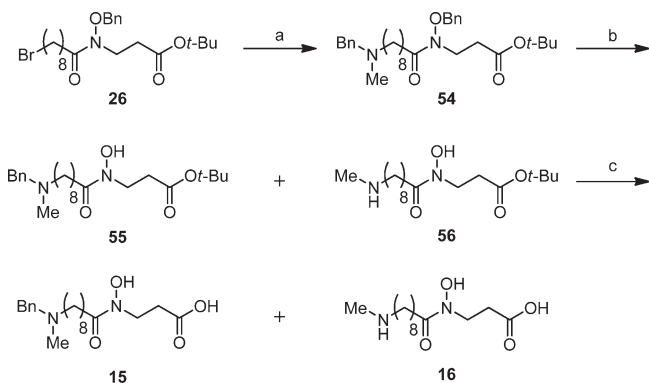
Having investigated the requirements for linker length, we next converted the hydroxamate of **8** to the retro-hydroxamate (compound **13**) for further structural optimization.

Scheme 5^a



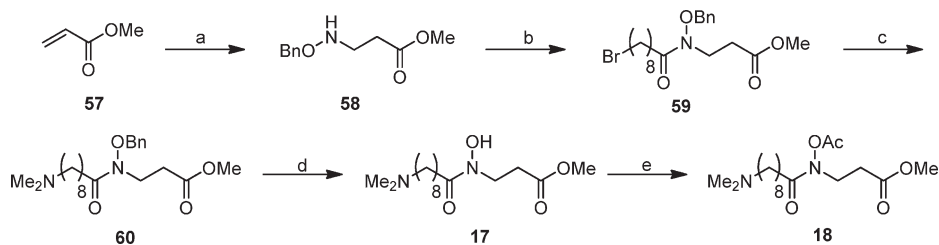
^a Reagents and conditions: (a) *n*-BuMeNH, MeCN, reflux, 80%; (b) H₂, Pd/C, AcOEt, room temp, 100%; (c) HCl, 1,4-dioxane, CH₂Cl₂, room temp, 72%.

Scheme 6^a



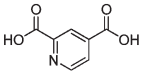
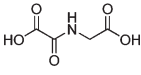
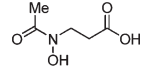
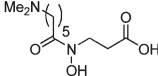
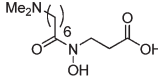
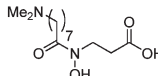
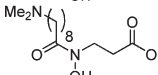
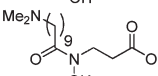
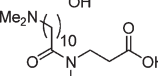
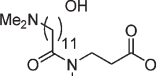
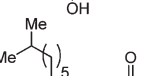
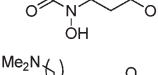
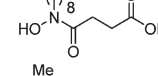
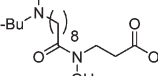
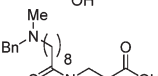
^a Reagents and conditions: (a) BnMeNH, MeCN, reflux, 74%; (b) H₂, Pd/C, AcOEt, room temp; (c) HCl, 1,4-dioxane, CH₂Cl₂, room temp, 26% for **15** and 37% for **16** (two steps).

Scheme 7^a



^a Reagents and conditions: (a) *O*-benzylhydroxylamine, Et₃N, 1,4-dioxane, reflux, 50% (b) 9-bromononanoyl chloride, Et₃N, DMAP, CH₂Cl₂, room temp, 56%; (c) Me₂NH, MeCN, reflux, 46%; (d) H₂, Pd/C, AcOEt, room temp, 96%; (e) AcCl, Et₃N, DMAP, CH₂Cl₂, room temp, 38%.

Table 1. In Vitro JMJD2C-, JMJD2A-, PHD1-, and PHD2-Inhibitory Activities of PCA (**1**), NOG (**2**), and Compounds **4–16**^a

compound	structure	IC ₅₀ (μM)			
		JMJD2C	JMJD2A	PHD1	PHD2
1		9.4	4.2	1.5	6.1
2		500	250	2.1	5.6
4		34	14	>100	>100
5		10	17	ND ^b	ND
6		2.7	8.7	ND	ND
7		1.5	6.0	>100	>100
8		1.0	3.0	>100	>100
9		1.6	5.5	>100	>100
10		5.2	11	ND	ND
11		8.8	22	ND	ND
12		74	120	ND	ND
13		2.0	8.1	>100	>100
14		1.5	3.2	>100	>100
15		1.3	2.0	ND	ND
16		1.7	4.4	ND	ND

^a Values are means of at least two experiments. ^b ND = No data.

However, this change decreased the JMJD2-inhibitory activity by 2-fold as compared with the parent compound **8**.

We next turned our attention to replacement of the dimethylamino group of compound **8**. The conversion of the dimethylamino group of **8** to other alkylamino groups (compounds **14–16**) slightly reduced or sustained the JMJD2-inhibitory activity.

As for the selectivity between JMJD2C and JMJD2A, while PCA (**1**) and NOG (**2**) inhibited JMJD2A rather than JMJD2C (JMJD2A IC₅₀/JMJD2C IC₅₀ for PCA (**1**) = 0.45; JMJD2A IC₅₀/JMJD2C IC₅₀ for NOG (**1**) = 0.50), compounds **4–16** inhibited JMJD2C in preference to JMJD2A (JMJD2A IC₅₀/JMJD2C IC₅₀ = 1.5–4.1). In particular, the

JMJD2C selectivity of compounds **7** and **13** is about 10 times higher than that of PCA (**1**) and NOG (**2**).

A selected set of compounds found to be active in the JMJD2 inhibition assay was further evaluated for PHD1- and PHD2-inhibitory activity (Table 1). Unexpectedly, while PCA (**1**) and NOG (**2**) inhibited both PHD1 and PHD2 with IC₅₀s in the micromolar range (IC₅₀ of 1.5–6.1 μM), compound **4** did not inhibit either prolyl hydroxylase PHD1 or PHD2, which are other Fe(II)/α-ketoglutarate-dependent enzymes (IC₅₀ > 100 μM), showing high selectivity for JMJD2 over PHD1 and PHD2. Furthermore, derivatives of compound **4** (compounds **7–9**, **13**, and **14**) displayed high selectivity for JMJD2 over PHD1 and PHD2 (PHD IC₅₀s > 100 μM).

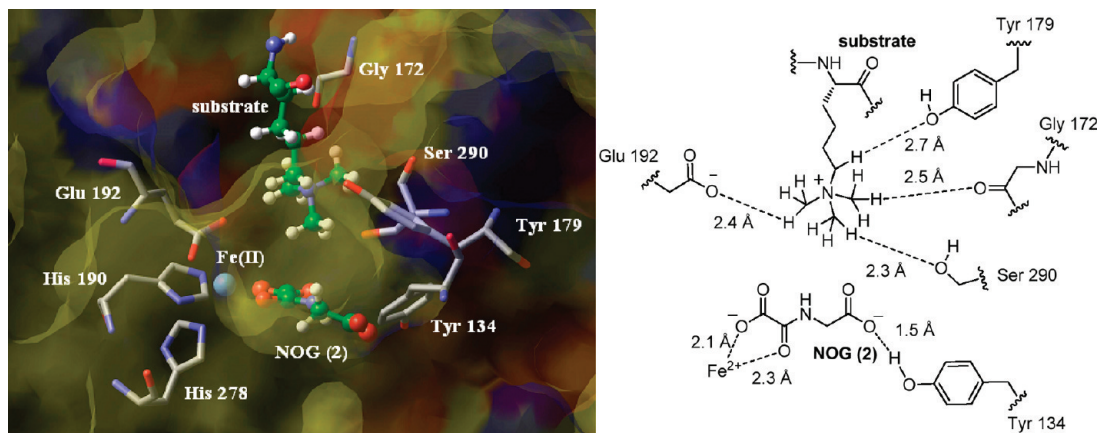


Figure 1. View of the active site of the JMJD2C homology model.

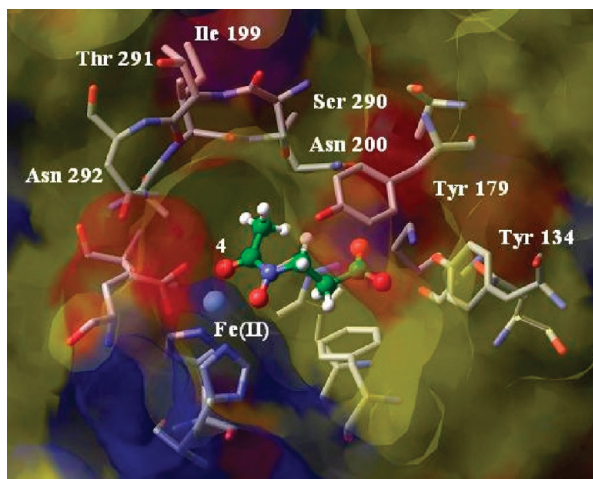


Figure 2. View of the conformation of compound **4** (ball-and-stick) docked in the JMJD2C active site.

Thus, compound **8** was the most potent and selective JMJD2 inhibitor in these enzyme assays.

Molecular Modeling. To explore the origin of the JMJD2 selectivity of compound **4** over PHDs, we initially performed a binding mode study of compound **4** with a homology model of JMJD2C. The low-energy conformation of **4** docked in a model based on the homology model of JMJD2C was calculated using MacroModel 8.1 software. Inspection of the simulated JMJD2C/compound **4** complex showed that the hydroxamate group of compound **4** coordinates to the Fe(II) bidentately, and the other carboxyl group forms a hydrogen bond with Tyr 134 in the active center of JMJD2C (Figure 2). In addition, the methyl group of compound **4** is located in the region delineated by Tyr 179, Asn 200, and Ser 290, where there appears to be no interaction between the methyl group and the amino acid residues. Compound **4** was calculated to bind JMJD2A in a binding mode similar to JMJD2A (Supporting Information Figure S3). On the other hand, compound **4** could not be docked in the active site of PHD2 because of a steric clash between the methyl group of **4** and Met 299 of PHD2. These results suggest that the methyl group attached to the carbonyl of the hydroxamate is important for the selectivity for JMJD2 over PHDs.

Next, we studied the binding mode of compound **8** in the active site of JMJD2C (Figure 3). As in the case of compound **4**, it appears that the hydroxamate group of compound **8** chelates Fe(II) in a bidentate fashion, and a hydrogen bond is

formed between the other carboxyl group and Tyr 134. In addition, the protonated dimethyl group lies in the hydrophilic region delineated by Asp 137, Gly 172, and Tyr 179, where the CH groups can interact with the amino acid residues via $\text{CH}\cdots\text{O}$ hydrogen bonds in addition to cation–dipole interactions. There also appears to be a hydrophobic interaction between the methylene groups of **8** and Val 173. The observed interactions between **8** and JMJD2C suggest the importance in potency of the tertiary amino group and the linker length of the inhibitor for the interaction.

Cellular Assays. To explore the potential of JMJD2 inhibitors as anticancer drugs, we tested compound **8**, the most selective and active compound in this series, by means of cancer cell growth inhibition assay using human prostate cancer LNCaP cells, which express JMJD2C.⁶ In addition to compound **8**, compounds **17** and **18** (Scheme 6), prodrugs of compound **8**, and a dimethylester prodrug of PCA (**1**) (DMPCA, **61**) (Chart 2) were used for the cellular study because these compounds were expected to permeate the cell membrane more efficiently than the parent compound and to be converted to **8** or PCA (**1**) by enzymatic hydrolysis within the cell.¹⁶ However, compounds **8**, **17**, **18**, and DMPCA (**61**) were found to be inactive at concentrations up to 100 μM . On the basis of the report that JMJD2C demethylates trimethylated Lys 9 of histone H3 cooperatively with LSD1 and is involved in the regulation of gene expression,⁶ we next evaluated whether our JMJD2 inhibitor could act synergistically with NCL-2 (**62**) (Chart 2), an LSD1-selective inhibitor discovered by us,¹⁷ in growth inhibition assay using LNCaP cells. Because NCL-2 (**62**) exerts a cancer cell growth-inhibitory effect by inhibiting LSD1,¹⁷ we considered that the combination of our JMJD2 inhibitor and NCL-2 (**62**) might cause a synergistic inhibition of cancer cell growth. As shown in Figure 4, 30 μM **8**, **17**, **18**, or DMPCA (**61**) did not show any activity as a single agent, while treatment with NCL-2 (**62**) reduced the cell growth with a GI_{50} value of 36 μM . As we had hoped, a combination of 30 μM prodrug **17** or **18**, or DMPCA (**61**), with NCL-2 (**62**) reduced the cell growth, as compared with NCL-2 (**62**) alone. Compounds **17** and **18** were more effective than DMPCA (**61**). Further, we examined the effects on other cancer cell lines. Curiously, compound **17** or **18** did not affect esophageal cancer KYSE150 cells (Supporting Information Figure S4), whereas the combination of NCL-2 (**62**) and compound **17** or **18** displayed synergistic cell growth inhibition of prostate cancer PC3 cells and colon cancer HCT116 cells, as in the case of LNCaP cells (Supporting Information Figures S5 and S6).

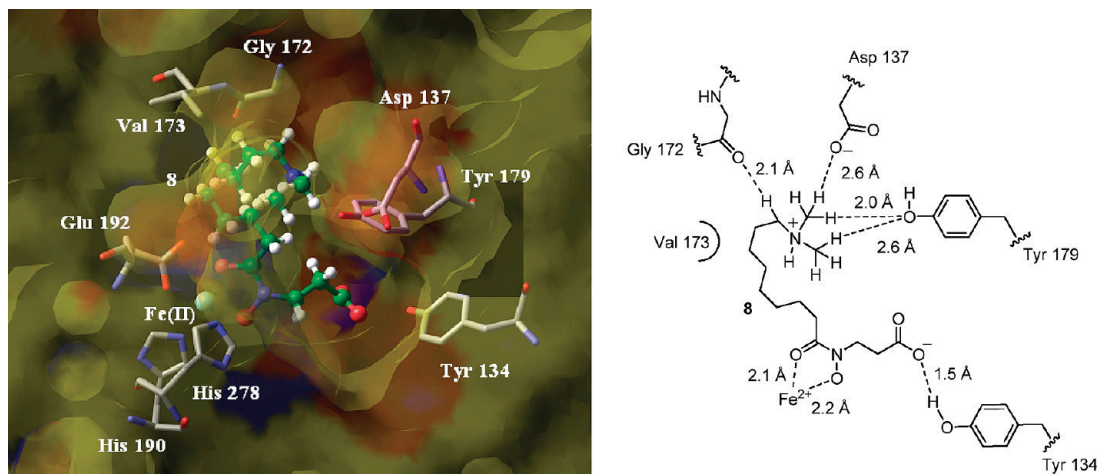


Figure 3. View of the conformation of compound **8** (ball-and-stick) docked in the JMJD2C catalytic core.

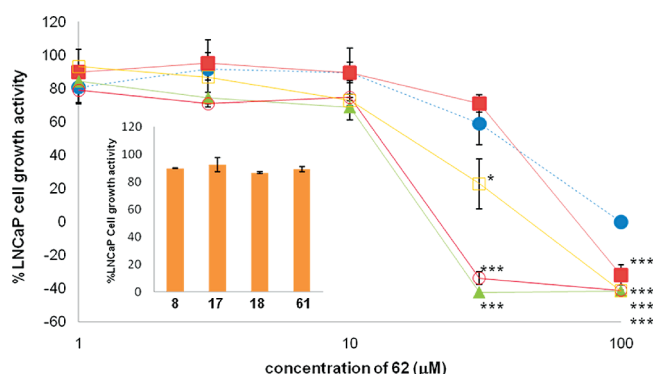
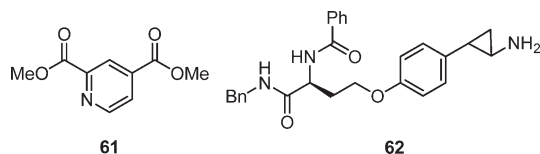


Figure 4. Growth inhibition of LNCaP cells by combinations of **8**, **17**, **18**, or **61** ($30 \mu\text{M}$) with the LSD1 inhibitor NCL-2 (**62**). Solid blue circles, **62** alone; Solid red squares, combination of **62** and **8**; Solid green triangles, combination of **62** and **17**; open red circles, combination of **62** and **18**; open gold squares, combination of **62** and **61**. Bar graphs show that single-agent administration of $30 \mu\text{M}$ **8**, **17**, **18**, or **61** does not affect the growth of LNCaP cells. *** $P < 0.001$; * $P < 0.05$; ANOVA and Bonferroni-type multiple t test.

Chart 2. Structures of DMPCA (**61**) and NCL-2 (**62**)



Therefore, cytotoxicity of JMJD2 inhibitors appears to be cell type-specific. These results indicate that a JMJD2 acts cooperatively with LSD1 in the expression of genes related to cell growth in LNCaP cells, PC3 cells, and HCT116 cells and is involved in the growth of the cancer cells. The use of JMJD2 inhibitors in combination with LSD1 inhibitors may have clinical potential for anticancer chemotherapy.

Conclusion

We have designed and synthesized novel JMJD2 inhibitors based on the crystal structure of JMJD2A and a homology model of JMJD2C complexed with NOG (**2**) and histone trimethylated lysine peptide. Compound **8** showed potent and selective JMJD2 inhibition in enzyme assays, showing 500-fold greater JMJD2C-inhibitory activity and more than 9100-fold greater JMJD2C-selectivity over PHDs, as compared

with the lead compound NOG (**2**). Preliminary SAR study and molecular modeling suggested that the methyl or methylene group next to the carbonyl of the hydroxamate is crucial for the JMJD2 selectivity, and the tertiary amino group and linker length are important for potent inhibition of JMJD2. In biological experiments, the combination of compound **17** or **18** (prodrugs of **8**) and the LSD1 inhibitor NCL-2 (**62**) synergistically inhibited cancer cell growth. These results suggest that JMJD2 inhibitors may be effective as antiproliferative and anticancer drugs when used in combination with LSD1 inhibitors. As far as we could determine, this is the first report to describe a cell-active JMJD-selective inhibitor. We believe this work should lead to the development of new tools for probing the biology of specific JMJD isoforms and may provide a new strategy for cancer treatment.

Experimental Section

Chemistry. Melting points were determined using a Yanagimoto micro melting point apparatus or a Büchi 545 melting point apparatus and were left uncorrected. Proton nuclear magnetic resonance spectra (^1H NMR) and carbon nuclear magnetic resonance spectra (^{13}C NMR) were recorded on JEOL JNM-LA500, JEOL JNM-A500, or BRUKER AVANCE600 spectrometers in the indicated solvent. Chemical shifts (δ) are reported in parts per million relative to the internal standard tetramethylsilane. Elemental analysis was performed with a Yanaco CHN CORDER NT-5 analyzer, and all values were within $\pm 0.4\%$ of the calculated values and these statement confirming $>95\%$ purity. High-resolution mass spectra (HRMS) and fast atom bombardment (FAB) mass spectra were recorded on a JEOL JMS-SX102A mass spectrometer. Purity testing was done by means of analytical HPLC on a Shimadzu instrument equipped with an Inertsil ODS-3 column ($4.6 \text{ mm} \times 150 \text{ mm}$, GL Science) eluted at 1 mL/min with Milli-Q water and CH_3CN . All tested compounds were $\geq 95\%$ pure. Preparative HPLC was performed with a Jasco instrument equipped with an Inertsil ODS-3 column ($20 \text{ mm} \times 250 \text{ mm}$, GL Science) eluted at 10 mL/min with Milli-Q water and CH_3CN . The absorbance of the tested compounds was measured at 213 nm . Gradient conditions of HPLC were as follows (A, CH_3CN containing 0.1% TFA; B, Milli-Q water); gradient (I), A 0% (0 to 2 min), A 0% to A 20% (2 to 20 min), A 20% (20 to 30 min), A 20% to A 0% (30 to 35 min), and A 0% (35 to 40 min); gradient (II), A 2% (0 to 2 min), A 2% to A 50% (2 to 20 min), A 50% (20 to 30 min), A 50% to A 2% (30 to 35 min), and A 2% (35 to 40 min). Reagents and solvents were purchased from Aldrich, Tokyo Kasei Kogyo, Wako Pure Chemical Industries, and Kanto Kagaku and used without purification.

Flash column chromatography was performed using silica gel 60 (particle size 0.046–0.063 mm) supplied by Merck.

3-[Acetyl(hydroxy)amino]propanoic Acid (4). Step 1: Preparation of *tert*-Butyl 3-(benzyloxyamino)propanoate (20). A solution of **19** (8.16 g, 63.2 mmol), benzyloxyamine hydrochloride (2.37 g, 14.8 mmol), and Et₃N (4 mL) in dioxane (30 mL) was stirred at reflux temperature for 32 h. The reaction mixture was poured into water and extracted with AcOEt. The organic layer was washed with brine and dried over Na₂SO₄. Filtration, concentration in vacuo, and purification by silica gel flash column chromatography (AcOEt/*n*-hexane = 1/10) gave 1.63 g (44%) of **20** as a yellow oil. ¹H NMR (CDCl₃, 500 MHz, δ, ppm) 7.35 (5H, m), 5.82 (1H, broad s), 4.70 (2H, s), 3.17 (2H, t, *J* = 6.4 Hz), 2.49 (2H, t, *J* = 6.4 Hz), 1.44 (9H, s).

Step 2: Preparation of *tert*-Butyl 3-[acetyl(benzyloxy)amino]propanoate (21). To a solution of **20** (1.24 g, 4.93 mmol) obtained above, Et₃N (1 mL, 7.18 mmol), and a catalytic amount of DMAP in 25 mL of CH₂Cl₂ was added dropwise a solution of acetyl chloride (1.41 g, 18.0 mmol) in 5 mL of CH₂Cl₂. After 15 min, the reaction mixture was poured into water and extracted with AcOEt. The organic layer was washed with brine and dried over Na₂SO₄. Filtration, concentration in vacuo, and purification by silica gel flash column chromatography (AcOEt/*n*-hexane = 1/4) gave 1.30 g (90%) of **21** as a colorless oil. ¹H NMR (CDCl₃, 500 MHz, δ, ppm) 7.38 (5H, m), 4.83 (2H, s), 3.92 (2H, t, *J* = 6.7 Hz), 2.54 (2H, t, *J* = 7.3 Hz), 2.07 (3H, s), 1.42 (9H, s).

Step 3: Preparation of *tert*-Butyl 3-[acetyl(hydroxy)amino]propanoate (22). To a solution of **21** (726 mg, 2.47 mmol) obtained above in 3 mL of AcOEt was added 354 mg of 5% Pd/C. The mixture was stirred under H₂ at room temperature for 4 h, then filtered through Celite. The filtrate was concentrated in vacuo and purified by silica gel flash column chromatography (AcOEt/*n*-hexane = 1/1) to give 402 mg (80%) of **22** as a colorless oil. ¹H NMR (CDCl₃, 500 MHz, δ, ppm) 3.87 (2H, m), 2.65 (2H, t, *J* = 6.1 Hz), 2.18 and 2.15 (3H, each s), 1.46 (9H, s).

Step 4: Preparation of 3-[Acetyl(hydroxy)amino]propanoic acid (4). To a solution of **22** (109 mg, 0.536 mmol) obtained above in 3 mL of CH₂Cl₂ was added TFA (0.5 mL, 7.91 mmol), and the mixture was stirred at room temperature for 5 h. Concentration in vacuo and purification by silica gel flash column chromatography (AcOEt only) gave 60 mg (76%) of **4** as a colorless oil. ¹H NMR (DMSO-*d*₆, 500 MHz, δ, ppm) 9.78 (1H, broad s), 4.10 (2H, t, *J* = 5.2 Hz), 2.45 (2H, t, *J* = 7.0 Hz), 1.96 (3H, s). ¹³C NMR (CD₃OD, 150 MHz, δ, ppm) 175.2, 173.8, 45.0, 32.4, 20.2. MS (FAB) *m/z* 148 (MH⁺). HRMS calcd for C₅H₁₀NO₄, 148.0613; found, 148.0610. HPLC *t*_R = 13.08 min (gradient I), purity 96.8%.

3-[[6-(Dimethylamino)hexanoyl](hydroxy)amino]propanoic Acid Hydrochloride (5·HCl). Step 1: Preparation of *tert*-Butyl 3-[(benzyloxy)(6-bromohexanoyl)amino]propanoate (23). To a solution of **20** (140 mg, 0.557 mmol), Et₃N (1 mL, 7.18 mmol), and a catalytic amount of DMAP in 10 mL of CH₂Cl₂ was added dropwise a solution of 6-bromohexanoyl chloride (391 mg, 1.84 mmol) in 5 mL of CH₂Cl₂. After 30 min, the reaction mixture was poured into water and extracted with AcOEt. The organic layer was washed with brine and dried over Na₂SO₄. Filtration, concentration in vacuo, and purification by silica gel flash column chromatography (AcOEt/*n*-hexane = 1/3) gave 114 mg (47%) of **23** as a yellow oil. ¹H NMR (CDCl₃, 500 MHz, δ, ppm) 7.38 (5H, m), 4.82 (2H, s), 3.92 (2H, t, *J* = 7.0 Hz), 3.39 (2H, t, *J* = 7.6 Hz), 2.53 (2H, t, *J* = 7.6 Hz), 2.35 (2H, t, *J* = 7.3 Hz), 1.84 (2H, quintet, *J* = 7.3 Hz), 1.59 (2H, quintet, *J* = 7.9 Hz), 1.42 (11H, m).

Step 2: Preparation of *tert*-Butyl 3-[(Benzyloxy)[6-(dimethylamino)hexanoyl]amino]propanoate (30). A solution of **23** (1.09 g, 2.37 mmol) obtained above, 50% aqueous solution of dimethylamine (1.10 g, 8.16 mmol), and Et₃N (1 mL, 7.18 mmol) in dioxane (20 mL) was stirred at reflux temperature for 9 h. The reaction mixture was poured into water and extracted with AcOEt. The organic layer was washed with brine and dried over Na₂SO₄. Filtration, concentration in vacuo, and purification by

silica gel flash column chromatography (CHCl₃/MeOH = 10/1) gave 492 mg (49%) of **30** as a yellow oil. ¹H NMR (CDCl₃, 500 MHz, δ, ppm) 7.47 (5H, m), 4.82 (2H, s), 3.91 (2H, t, *J* = 6.7 Hz), 2.52 (3H, t, *J* = 7.0 Hz), 2.36 (2H, t, *J* = 7.6 Hz), 2.32 (6H, broad s), 1.59 (2H, quintet, *J* = 7.6 Hz), 1.54 (2H, m), 1.47 (2H, quintet, *J* = 7.0 Hz), 1.42 (9H, s), 1.30 (2H, quintet, *J* = 7.3 Hz).

Steps 3 and 4: Preparation of 3-[[6-(Dimethylamino)hexanoyl](hydroxy)amino]propanoic Acid Hydrochloride (5·HCl). Compound **5·HCl** was prepared from **30** obtained above using the procedure described for **4** (steps 3 and 4) in 42% yield as a colorless amorphous solid. ¹H NMR (DMSO-*d*₆, 500 MHz, δ, ppm) 9.74 (1H, broad s), 9.52 (1H, m), 3.71 (2H, t, *J* = 7.3 Hz), 3.00 (2H, m), 2.74 (6H, d, *J* = 4.9 Hz), 2.45 (2H, t, *J* = 7.3 Hz), 2.35 (2H, t, *J* = 7.3 Hz), 1.60 (2H, quintet, *J* = 7.3 Hz), 1.51 (2H, quintet, *J* = 7.6 Hz), 1.28 (2H, quintet, *J* = 8.2 Hz). ¹³C NMR (CD₃OD, 125 MHz, δ, ppm) 175.79, 175.10, 58.85, 45.20, 43.42, 32.71, 32.47, 26.91, 25.32, 24.96. MS (FAB) *m/z* 247 (MH⁺ - HCl). HRMS calcd for C₁₁H₂₃N₂O₄, 247.1660; found, 247.1658. HPLC *t*_R = 12.90 min (gradient I), purity 95.2%.

3-[[7-(Dimethylamino)heptanoyl](hydroxy)amino]propanoic Acid Hydrochloride (6·HCl). Step 1: Preparation of *tert*-Butyl 3-[(Benzyloxy)(7-bromoheptanoyl)amino]propanoate (24). To a solution of 7-bromoheptanoic acid (3.15 g, 15.1 mmol) and oxalyl chloride (8.12 g, 64.5 mmol) in 30 mL of CH₂Cl₂ was added a catalytic amount of DMF. The mixture was stirred at room temperature for 2 h. Removal of the solvent in vacuo gave 7-bromoheptanoic acid chloride as a colorless oil.

To a solution of **20** (2.90 g, 11.5 mmol), Et₃N (3 mL, 21.5 mmol), and a catalytic amount of DMAP in 50 mL of CH₂Cl₂ was added dropwise a solution of 7-bromoheptanoic acid chloride obtained above in 10 mL of CH₂Cl₂. After 15 min, the reaction mixture was poured into water and extracted with AcOEt. The organic layer was washed with brine and dried over Na₂SO₄. Filtration, concentration in vacuo, and purification by silica gel flash column chromatography (AcOEt/*n*-hexane = 1/5) gave 3.02 g (59%) of **24** as a yellow oil. ¹H NMR (CDCl₃, 500 MHz, δ, ppm) 7.38 (5H, m), 4.82 (2H, s), 3.92 (2H, m), 2.53 (2H, t, *J* = 7.0 Hz), 2.35 (2H, t, *J* = 7.6 Hz), 1.84 (3H, t, *J* = 7.3 Hz), 1.58 (3H, t, *J* = 7.9 Hz), 1.42 (11H, m), 1.30 (2H, quintet, *J* = 7.6 Hz).

Steps 2, 3, and 4: Preparation of 3-[[7-(Dimethylamino)heptanoyl](hydroxy)amino]propanoic Acid Hydrochloride (6·HCl). Compound **6·HCl** was prepared from **24** obtained above using the procedure described for **5** (step 2) and **4** (steps 3 and 4) in 19% yield as a colorless amorphous solid. ¹H NMR (DMSO-*d*₆, 500 MHz, δ, ppm) 10.09 (1H, broad s), 9.77 (1H, broad s), 3.70 (2H, t, *J* = 7.3 Hz), 2.99 (2H, m), 2.72 (6H, d, *J* = 4.8 Hz), 2.46 (2H, t, *J* = 6.7 Hz), 2.34 (2H, t, *J* = 7.3 Hz), 1.62 (2H, quintet, *J* = 7.6 Hz), 1.49 (2H, quintet, *J* = 6.7 Hz), 1.28 (2H, m). ¹³C NMR (DMSO-*d*₆, 150 MHz, δ, ppm) 172.81, 172.61, 69.68, 56.29, 45.91, 43.39, 41.79, 33.41, 31.50, 31.44, 28.21, 28.08, 27.88, 25.62, 25.53, 23.33, 22.31. MS (FAB) *m/z* 261 (MH⁺ - HCl). HRMS calcd for C₁₂H₂₅N₂O₄, 261.1806; found, 261.1814. HPLC *t*_R = 14.76 min (gradient I), purity 95.2%.

Compounds **7–11** were prepared from **20** and an appropriate carboxylic acid using the procedure described for **6**.

3-[[8-(Dimethylamino)octanoyl](hydroxy)amino]propanoic Acid Hydrochloride (7·HCl). Yield 47%; colorless crystals; mp 64–67 °C. ¹H NMR (DMSO-*d*₆, 600 MHz, δ, ppm) 9.72 (1H, broad s), 9.41 (1H, broad s), 3.70 (2H, t, *J* = 7.2 Hz), 3.00 (2H, m), 2.75 (6H, d, *J* = 4.8 Hz), 2.45 (2H, m), 2.33 (2H, t, *J* = 7.8 Hz), 1.59 (2H, m), 1.48 (2H, m), 1.28 (6H, m). ¹³C NMR (CD₃OD, 125 MHz, δ, ppm) 172.57, 56.49, 45.99, 43.48, 41.97, 33.57, 31.60, 28.45, 28.25, 28.12, 25.70, 24.30, 23.93, 23.52. MS (FAB) *m/z* 275 (MH⁺ - HCl). HRMS calcd for C₁₃H₂₇N₂O₄, 275.1970; found, 275.1971. HPLC *t*_R = 19.91 min (gradient I), purity 96.8%.

3-[[9-(Dimethylamino)nonanoyl](hydroxy)amino]propanoic Acid Hydrochloride (8·HCl). Yield 46%; colorless crystals; mp 72–74 °C. ¹H NMR (DMSO-*d*₆, 600 MHz, δ, ppm) 9.71 (2H, m), 3.70 (2H, t, *J* = 7.2 Hz), 3.00 (2H, t, *J* = 7.8 Hz), 2.72 (6H, s), 2.45 (2H, m), 2.32 (2H, t, *J* = 7.2 Hz), 1.61 (2H, m), 1.48 (2H, m),

1.27 (8H, m). ^{13}C NMR (DMSO- d_6 , 125 MHz, δ , ppm) 172.92, 172.52, 56.35, 43.38, 41.83, 31.57, 31.49, 28.53, 28.48, 28.24, 25.74, 23.94, 23.45. MS (FAB) m/z 289 ($\text{MH}^+ - \text{HCl}$). HRMS calcd for $\text{C}_{14}\text{H}_{29}\text{N}_2\text{O}_4$, 289.2126; found, 289.2127. HPLC $t_{\text{R}} = 20.96$ min (gradient (I), purity 95.0%).

3-[[10-(Dimethylamino)decanoyl](hydroxy)amino]propanoic Acid Hydrochloride (9·HCl). Yield 46%; a colorless amorphous solid. ^1H NMR (DMSO- d_6 , 150 MHz, δ , ppm) 9.66 (1H, broad s), 9.19 (1H, broad s), 3.70 (2H, t, $J = 7.2$ Hz), 3.01 (2H, m), 2.76 (6H, d, $J = 4.8$ Hz), 2.44 (2H, m), 2.32 (2H, t, $J = 7.2$ Hz), 1.58 (2H, m), 1.47 (2H, m), 1.26 (10H, m). ^{13}C NMR (DMSO- d_6 , 600 MHz, δ , ppm) 174.38, 172.52, 56.53, 43.38, 42.03, 33.55, 31.56, 31.47, 28.63, 28.53, 25.68, 24.37, 23.99, 23.55. MS (FAB) m/z 303 ($\text{MH}^+ - \text{HCl}$). HRMS calcd for $\text{C}_{15}\text{H}_{31}\text{N}_2\text{O}_4$, 303.2281; found, 303.2284. HPLC $t_{\text{R}} = 15.11$ min (gradient (II), purity 96.5%).

3-[[11-(Dimethylamino)undecanoyl](hydroxy)amino]propanoic Acid Hydrochloride (10·HCl). Yield 87%; a yellow amorphous solid. ^1H NMR (DMSO- d_6 , 150 MHz, δ , ppm) 9.65 (1H, broad s), 9.23 (1H, broad s), 3.70 (2H, t, $J = 7.2$ Hz), 3.01 (2H, m), 2.75 (6H, d, $J = 4.8$ Hz), 2.44 (2H, m), 2.31 (2H, t, $J = 7.2$ Hz), 1.58 (2H, m), 1.47 (2H, m), 1.26 (12H, m). ^{13}C NMR (DMSO- d_6 , 125 MHz, δ , ppm) 173.15, 172.68, 56.67, 42.15, 42.12, 31.71, 31.62, 28.77, 28.48, 25.83, 24.13, 23.66. MS (FAB) m/z 317 ($\text{MH}^+ - \text{HCl}$). HRMS calcd for $\text{C}_{16}\text{H}_{33}\text{N}_2\text{O}_4$, 317.2435; found, 317.2440. HPLC $t_{\text{R}} = 16.03$ min (gradient (II), purity 95.0%).

3-[[12-(Dimethylamino)dodecanoyl](hydroxy)amino]propanoic Acid Hydrochloride (11·HCl). Yield 7.9%; a yellow amorphous solid. ^1H NMR (DMSO- d_6 , 600 MHz, δ , ppm) 9.65 (1H, broad s), 9.17 (1H, broad s), 3.70 (2H, t, $J = 7.2$ Hz), 3.01 (2H, m), 2.75 (6H, d, $J = 5.4$ Hz), 2.44 (2H, m), 2.31 (2H, t, $J = 7.2$ Hz), 1.58 (2H, quintet, $J = 6.6$ Hz), 1.46 (2H, m), 1.25 (14H, m). ^{13}C NMR (DMSO- d_6 , 125 MHz, δ , ppm) 175.18, 174.12, 59.21, 45.14, 43.45, 33.32, 32.63, 32.44, 30.53, 30.12, 27.46, 27.39, 25.85, 25.70, 25.65. MS (FAB) m/z 331 ($\text{MH}^+ - \text{HCl}$). HRMS calcd for $\text{C}_{17}\text{H}_{35}\text{N}_2\text{O}_4$, 331.2600; found, 331.2597. HPLC $t_{\text{R}} = 23.49$ min (gradient (II), purity 97.2%).

3-(*N*-Hydroxy-7-methyloctanamido)propanoic Acid (12). Steps 1 and 2: Preparation of *tert*-Butyl 3-[Benzyloxy(7-methyloctanoyl)amino]propanoate (45). To a solution of 7-methyloctanoic acid (44, 870 mg, 5.50 mmol) and oxalyl chloride (2.34 g, 18.4 mmol) in 8 mL of CH_2Cl_2 was added a catalytic amount of DMF. The mixture was stirred at room temperature for 45 min. Concentration in vacuo of the mixture gave the acid chloride of 44 as a colorless oil.

To a solution of 20 (1.81 g, 7.20 mmol), triethylamine (2 mL), and catalytic amount of DMAP in 25 mL of CH_2Cl_2 was added a solution of the acid chloride obtained above in 5 mL of CH_2Cl_2 in a dropwise fashion. The mixture was stirred at room temperature for 1 h. The reaction mixture was poured into water and extracted with AcOEt. The organic layer was separated and washed with 4N aqueous HCl and brine, and dried over Na_2SO_4 . Filtration, concentration in vacuo, and purification by silica gel flash column chromatography (AcOEt/*n*-hexane = 1/10) gave 1.36 g (63%) of 45 as a colorless oil. ^1H NMR (CDCl_3 , 500 MHz, δ , ppm) 7.38 (5H, m), 4.82 (2H, s), 3.91 (2H, t, $J = 5.8$ Hz), 2.53 (2H, t, $J = 7.0$ Hz), 2.35 (2H, t, $J = 7.9$ Hz), 1.56 (3H, t, $J = 7.6$ Hz), 1.52 (1H, septet, $J = 6.7$ Hz), 1.41 (9H, s), 1.27 (4H, m), 1.15 (2H, m), 0.85 (2H, d, $J = 6.4$ Hz).

Steps 3 and 4: Preparation of 3-(*N*-Hydroxy-7-methyloctanamido)propanoic acid (12). Compound 12 was prepared from 45 obtained above using the procedure described for 4 (steps 3 and 4) in 38% yield as colorless crystals: mp 66–68 °C. ^1H NMR (DMSO- d_6 , 500 MHz, δ , ppm) 3.70 (2H, t, $J = 7.0$ Hz), 2.45 (2H, t, $J = 7.3$ Hz), 2.31 (2H, t, $J = 7.3$ Hz), 1.53–1.46 (3H, m), 1.25–1.24 (4H, m), 1.16–1.12 (2H, m), 0.85 (6H, d, $J = 6.7$ Hz). ^{13}C NMR (DMSO- d_6 , 125 MHz, δ , ppm) 173.13, 172.66, 43.51, 38.36, 31.70, 31.58, 29.06, 27.39, 26.64, 24.17, 22.53. MS (FAB) m/z 246 ($\text{M}^+ + 1$). Anal. Calcd for $\text{C}_{12}\text{H}_{23}\text{NO}_4$: C, 58.75; H, 9.45; N, 5.71. Found: C, 58.51; H, 9.22; N, 5.86.

***tert*-Butyl 4-[(8-Dimethylamino)octyl](hydroxy)amino]-4-oxobutanoic Acid Hydrochloride (13·HCl)**. Step 1: Preparation of *tert*-Butyl 4-[(Benzyloxy)amino]-4-oxobutanoate (48). A solution

of 47 (2.03 g, 11.6 mmol), benzyloxyamine (2.27 g, 18.4 mmol), EDCI (4.89 g, 25.5 mmol), and $\text{HOBt} \cdot \text{H}_2\text{O}$ (3.75 g, 24.5 mmol) in DMF (50 mL) was stirred at room temperature for 16 h. The reaction mixture was poured into water and extracted with AcOEt. The organic layer was washed with brine and dried over Na_2SO_4 . Filtration, concentration in vacuo, and purification by silica gel flash column chromatography (AcOEt/*n*-hexane = 1/3) gave 1.27 g (39%) of 48 as a colorless oil. ^1H NMR (CDCl_3 , 500 MHz, δ , ppm) 8.41 (1H, broad s), 7.39 (5H, m), 4.90 (2H, s), 2.58 (2H, m), 2.17 (2H, m), 1.44 (9H, s).

Step 2: Preparation of *tert*-Butyl 4-[(benzyloxy)(8-bromooctyl)amino]-4-oxobutanoate (49). A mixture of 48 (640 mg, 2.29 mmol) obtained above and 60% NaH in oil (180 mg, 4.50 mmol) in DMF (30 mL) was stirred at room temperature for 30 min. To the mixture was added dropwise 1,4-dibromooctane (2.14 g, 7.50 mmol), and the mixture was stirred at 50 °C for 3 h. Then, the reaction mixture was poured into water and extracted with AcOEt. The organic layer was washed with brine and dried over Na_2SO_4 . Filtration, concentration in vacuo, and purification by silica gel flash column chromatography (AcOEt/*n*-hexane = 1/5) gave 455 mg (42%) of 49 as a colorless oil. ^1H NMR (CDCl_3 , 600 MHz, δ , ppm) 7.39 (5H, m), 4.86 (2H, s), 3.62 (2H, m), 3.39 (2H, t, $J = 6.6$ Hz), 2.70 (2H, m), 2.54 (2H, t, $J = 7.2$ Hz), 1.83 (2H, quintet, $J = 7.8$ Hz), 1.62 (2H, quintet, $J = 6.6$ Hz), 1.45 (9H, s), 1.40 (2H, quintet, $J = 7.2$ Hz), 1.29 (6H, m).

Steps 3, 4, and 5: Preparation of 4-[(8-Dimethylamino)octyl](hydroxy)amino]-4-oxobutanoic Acid Hydrochloride (13·HCl). Compound 13·HCl was prepared from 49 obtained above using the procedure described for 5 (step 2) and 4 (steps 3 and 4) in 14% yield as a colorless oil. ^1H NMR (DMSO- d_6 , 600 MHz, δ , ppm) 9.61 (1H, broad s), 9.18 (1H, broad s), 3.47 (2H, t, $J = 7.2$ Hz), 3.01 (2H, m), 2.76 (6H, d, $J = 5.4$ Hz), 2.58 (2H, t, $J = 7.2$ Hz), 2.39 (2H, t, $J = 7.2$ Hz), 1.58 (2H, m), 1.51 (2H, quin, $J = 6.6$ Hz), 1.28 (8H, m). ^{13}C NMR (DMSO- d_6 , 150 MHz, δ , ppm) 173.83, 56.55, 42.08, 28.22, 26.94, 26.08, 25.78, 25.57, 23.51. MS (FAB) m/z 289 ($\text{MH}^+ - \text{HCl}$). HRMS calcd for $\text{C}_{13}\text{H}_{29}\text{N}_2\text{O}_4$, 289.2125; found, 289.2127. HPLC $t_{\text{R}} = 13.32$ min (gradient (II), purity 99.3%).

3-[(9-Butyl(methyl)amino)nonanoyl](hydroxy)amino]propanoic Acid Hydrochloride (14·HCl). Compound 14 was prepared from 26 and butylmethylamine using the procedure described for 5 in 58% yield as a colorless amorphous solid. ^1H NMR (DMSO- d_6 , 600 MHz, δ , ppm) 9.67 (1H, broad s), 9.08 (1H, broad s), 3.70 (2H, t, $J = 7.2$ Hz), 3.07 (2H, m), 2.97 (2H, m), 2.73 (3H, d, $J = 4.8$ Hz), 2.46 (2H, m), 2.32 (2H, t, $J = 7.8$ Hz), 1.58 (4H, m), 1.48 (2H, quintet, $J = 6.6$ Hz), 1.27 (10H, m), 0.91 (3H, t, $J = 7.2$ Hz). ^{13}C NMR (DMSO- d_6 , 125 MHz, δ , ppm) 172.96, 172.51, 54.90, 54.67, 43.42, 31.56, 31.48, 28.54, 28.51, 28.24, 25.77, 25.21, 23.96, 23.18, 19.19, 13.38. MS (FAB) m/z 331 ($\text{MH}^+ - \text{HCl}$). HRMS calcd for $\text{C}_{16}\text{H}_{35}\text{N}_2\text{O}_4$, 331.2598; found, 331.2597. HPLC $t_{\text{R}} = 16.00$ min (gradient (II), purity 96.5%).

3-[(9-Benzyloxy(methyl)amino)nonanoyl](hydroxy)amino]propanoic Acid Hydrochloride (15·HCl) and 3-[(9-Hydroxy(9-methylamino)nonanoyl)]amino]propanoic Acid Hydrochloride (16·HCl). Step 1: Preparation of *tert*-Butyl 3-[(9-Benzyloxy(methyl)amino)nonanoyl](benzyloxy)amino]propanoate (54). A solution of 26 (140 mg, 0.298 mmol) obtained above and benzyloxyamine (370 mg, 3.05 mmol) in MeCN (5 mL) was stirred at reflux temperature for 12 h. The reaction mixture was poured into water and extracted with AcOEt. The organic layer was washed with brine and dried over Na_2SO_4 . Filtration, concentration in vacuo, and purification by silica gel flash column chromatography ($\text{CHCl}_3/\text{MeOH} = 30/1$) gave 113 mg (74%) of 54 as a yellow oil. ^1H NMR (CDCl_3 , 600 MHz, δ , ppm) 7.38–7.29 (10H, m), 4.82 (2H, s), 3.91 (2H, m), 2.53 (2H, t, $J = 6.6$ Hz), 2.33 (4H, t, $J = 7.8$ Hz), 2.17 (3H, s), 1.56 (2H, m), 1.49 (2H, m), 1.42 (9H, s), 1.26 (8H, m).

Step 2: Preparation of 3-[(9-Benzyloxy(methyl)amino)nonanoyl](hydroxy)amino]propanoic Acid Hydrochloride (15·HCl) and *tert*-Butyl 3-[(9-Hydroxy(9-methylamino)nonanoyl)]amino]propanoic Acid Hydrochloride (16·HCl). To a solution of 54 (112 mg, 0.219 mmol) obtained above in 5 mL of AcOEt was added 61 mg of 5% Pd/C. The mixture was stirred at room

temperature for 2 h under H₂, and then filtered. The filtrate was concentrated in vacuo to give 99 mg of a mixture of **55** and **56**.

To a solution of the mixture of **55** and **56** (99 mg) obtained above in 6 mL of CH₂Cl₂ was added 4 N HCl in dioxane (1 mL, 4.00 mmol) with cooling in an ice-bath, and the mixture was stirred at room temperature for 5 h. Concentration in vacuo gave a colorless amorphous solid. The amorphous solid was purified by HPLC (gradient (II)) to give 23 mg (26%) of **15·HCl** as a colorless amorphous solid and 25 mg (37%) of **16·HCl** as a colorless amorphous solid. **15·HCl**: ¹H NMR (DMSO-*d*₆, 600 MHz, δ , ppm) 9.66 (1H, broad s), 9.38 (1H, broad s), 7.49 (5H, m), 4.38 (1H, m), 4.21 (1H, m), 3.70 (2H, t, $J = 7.2$ Hz), 3.07 (1H, m), 2.98 (1H, m), 2.67 (3H, d, $J = 4.8$ Hz), 2.45 (2H, m), 2.32 (2H, t, $J = 7.2$ Hz), 1.71–1.60 (2H, m), 1.48 (2H, m), 1.27 (8H, m). ¹³C NMR (CD₃OD, 125 MHz, δ , ppm) 176.27, 175.10, 132.11, 131.27, 130.87, 130.45, 60.90, 57.10, 45.19, 40.04, 33.16, 32.44, 30.13, 30.05, 29.84, 27.41, 25.67, 25.11. MS (FAB) m/z 365 (MH⁺ – HCl). HRMS calcd for C₂₀H₃₃N₂O₄, 365.2447; found, 365.2440. HPLC $t_R = 16.46$ min (gradient (II), purity 97.9%). **16·HCl**: ¹H NMR (CD₃OD, 600 MHz, δ , ppm) 3.86 (2H, t, $J = 7.2$ Hz), 2.97 (2H, t, $J = 7.2$ Hz), 2.69 (3H, s), 2.59 (2H, m), 2.45 (2H, t, $J = 7.2$ Hz), 1.66 (2H, quintet, $J = 7.2$ Hz), 1.60 (2H, m), 1.38 (8H, m). ¹³C NMR (CD₃OD, 150 MHz, δ , ppm) 173.83, 172.29, 56.95, 43.93, 41.57, 32.42, 30.84, 24.95, 24.78, 24.65, 24.51, 24.23, 23.41, 23.33, 23.11. MS (FAB) m/z 275 (MH⁺ – HCl). HRMS calcd for C₁₃H₂₇N₂O₄, 275.1969; found, 275.1971. HPLC $t_R = 12.53$ min (gradient (II), purity 97.9%).

Methyl 3-[[9-(Dimethylamino)nonanoyl](hydroxyamino)propanoate (17). **Steps 1, 2, 3, and 4: Preparation of Methyl 3-[[9-(Dimethylamino)nonanoyl](hydroxyamino)propanoate (17)**. Compound **17** was prepared from **57** using the procedures described for **4** (step 1), **6** (step 1), **5** (step 2), and **4** (step 3) in 12% yield as a colorless amorphous solid. ¹H NMR (CD₃OD, 500 MHz, δ , ppm) 3.87 (2H, t, $J = 7.0$ Hz), 3.66 (3H, s), 2.60 (2H, t, $J = 7.0$ Hz), 2.46–2.38 (4H, m), 2.30 (6H, s), 1.58 (2H, m), 1.51 (2H, quintet, $J = 7.0$ Hz), 1.34 (8H, m). ¹³C NMR (CD₃OD, 125 MHz, δ , ppm) 176.42, 175.65, 60.56, 52.25, 45.14, 32.48, 30.42, 30.36, 28.38, 27.95, 25.79. MS (FAB) m/z 303 (MH⁺). HRMS calcd for C₁₅H₃₁N₂O₄, 303.2281; found, 303.2284. HPLC $t_R = 14.97$ min (gradient (II), purity 98.9%).

Methyl 3-[[9-(Dimethylamino)nonanoyl](methoxyamino)propanoate (18·TFA). To a solution of **17** (112 mg, 0.370 mmol) obtained above, Et₃N (0.11 mL, 0.790 mmol) in 5 mL of CH₂Cl₂ was added dropwise a solution of AcCl (283 mg, 3.61 mmol) in 5 mL of CH₂Cl₂. After 45 min, the reaction mixture was poured into saturated aqueous NaHCO₃ and extracted with AcOEt. The organic layer was washed with brine and dried over Na₂SO₄. Filtration, concentration in vacuo, purification by silica gel flash column chromatography (CHCl₃/MeOH = 15/1), and preparative HPLC (gradient (II)) gave 60 mg (38%) of **18·TFA** as a colorless amorphous solid. ¹H NMR (CDCl₃, 600 MHz, δ , ppm) 4.00 (2H, m), 3.69 (3H, s), 3.12 (2H, m), 2.89 (6H, s), 2.64 (2H, m), 2.28 (2H, m), 2.20 (3H, s), 1.72 (2H, m), 1.61 (2H, m), 1.39 (8H, m). ¹³C NMR (CD₃OD, 125 MHz, δ , ppm) 171.29, 56.58, 51.43, 42.09, 31.48, 31.08, 28.42, 28.20, 25.63, 23.56, 18.11. MS (FAB) m/z 345 (MH⁺ – TFA). HRMS calcd for C₁₅H₃₁N₂O₄, 345.2390; found, 345.2390. HPLC $t_R = 16.65$ min (gradient (II), purity 95.2%).

Biology. Measurement of JMJD2C Activity. The JMJD2C activity was assessed by means of formaldehyde dehydrogenase (FDH)-coupled assay^{4,18} with some modifications. The substrate used was H3K9me3 peptide (Sigma-Aldrich Japan, Tokyo), a chemically synthesized histone H3 peptide (aa 7–14) that contains trimethylated lysine at position 9.

In the assay, the reaction mixture (0.1 mL) contained 20 mM HEPES-KOH, pH 7.5, 70 μ M (NH₄)₂Fe(SO₄)₂·6(H₂O), 50 μ M H3K9me3 peptide, 0.2 mM α -ketoglutaric acid, 2 mM ascorbic acid, 1 mM APAD⁺, 1 mM reduced glutathione, 0.1 mg/mL FDH, 0.1 mg/mL BSA, and various amounts of JMJD2C. The production of APADH was monitored for 30 min in a 96-well

plate (Nunc, Roskilde, Denmark) using the DTX 880 multi-mode detector (Beckman Coulter, Inc., Fullerton, CA) at the excitation wavelength of 370 nm and the emission wavelength of 465 nm at 25 °C. The enzyme activity was determined from the linear part of the reaction curve.

JMJD2C Inhibition Assay. JMJD2C-inhibitory activity was measured using 0.53 mg/mL enzyme. Test compounds were dissolved in DMSO. The final concentrations of DMSO in the reaction mixtures were less than 3.3%, and it was confirmed that 3.3% DMSO did not affect the JMJD2C activity. Reaction with DMSO alone was also done as a control. Reaction mixtures (94.6 μ L), containing all of the materials except H3K9me3 peptide and α -ketoglutaric acid, were preincubated for 5 min. Then the reactions were started by the addition of 5.4 μ L of a solution of 0.93 mM H3K9me3 peptide and 3.7 mM α -ketoglutaric acid. The enzyme activity was determined as described above. The ratio of the enzyme activity measured in the presence of inhibitor to that of the control was plotted against log [Inhibitor]. To confirm that the reduction of the JMJD2C activity by test compounds was not due to inhibition of the coupled enzyme FDH, we examined the effects of the test compounds on FDH activity. The reaction mixture (0.1 mL) contained 20 mM HEPES-KOH, pH 7.5, 50 μ M formaldehyde, 1 mM APAD⁺, 1 mM reduced glutathione, 0.1 mg/mL BSA, 0.1 mg/mL FDH, and a fixed concentration of 123 μ M test compound. The FDH activity was measured by monitoring APADH formation as described above. The FDH activity in the presence of test compounds was similar to that in the absence of the compounds.

JMJD2A Inhibition Assay. The JMJD2A activity was measured by the FDH-coupled assay as described for JMJD2C except that reactions were performed in a final volume of 30 μ L in 384-well plate (Nunc) and a final concentration of the JMJD2A was 0.37 mg/mL.

PHD Inhibition Assay. The inhibitory activities of the test compounds against PHD1 and PHD2 were assayed according to a method reported in ref 19 with some modifications (for details see Supporting Information). Recombinant human PHD1 and PHD2 were purified from Sf9 cell lysates and used for hydroxylation of biotinylated HIF-1 α 556–574 peptide coated on NeutrAvidin plates (Pierce). Hydroxylated peptide was quantified after incubation with purified VBC complex labeled with europium ((DELFI) labeling reagent, Perkin-Elmer) and addition of enhancer solution (Perkin-Elmer) by measuring time-resolved fluorescence with a Tecan infinite M200 plate reader.

Cell Growth Inhibition Assay. LNCaP, PC-3, HCT116, and KYSE150 cells were plated in 96-well plates at initial densities of 8000 (LNCaP) or 4000 (PC-3 and HCT116 and KYSE150) cells/well (50 μ L/well) and incubated at 37 °C. After 24 h, cells were exposed to test compounds by adding solutions (50 μ L/well) of compounds at various concentrations in RPMI1640 (LNCaP), DMEM (PC-3), McCoy's 5A (HCT116), and Ham's F12 medium (KYSE150) at 37 °C at 5% CO₂ for 72 h. Then 10 μ L of AlamarBlue was added to each well, and incubation was continued at 37 °C for 3 h. The fluorescence in each well was measured with a fluorometric plate reader (excitation at 530 nm, emission at 590 nm). Absorbance values of control wells (*C*) and test wells (*T*) were measured. Moreover, the absorbance of the test wells (*T*₀) was also measured at time 0 (addition of compounds). Using these measurements, cell growth inhibition (percentage of growth) by a test inhibitor at each concentration used was calculated as: % growth = 100[(*T* – *T*₀)/(*C* – *T*₀)], when *T* > *T*₀ and % growth = 100[(*T* – *T*₀)/*T*], when *T* < *T*₀.

Molecular Modeling. A homology model for JMJD2C complexed with histone H3 peptide trimethylated at Lys 9 and NOG (**2**) based on the crystal structure of JMJD2A (PDB ID 2OQ6) was built using the homology modeling module of the Molecular Operating Environment (MOE) (Chemical Computing Group Inc., Montreal, Quebec, Canada).

Docking and subsequent scoring were performed using MacroModel 8.1 software. The structures of compounds **4** and **8** bound to JMJD2C or JMJD2A were constructed by molecular mechanics (MM) energy minimization. The starting positions of compounds **4** and **8** were determined manually: the hydroxamate moiety of **4** and **8** was superimposed onto the oxalyl group of NOG (**2**). The conformations of compounds **4** and **8** in the active site were minimized by MM calculation based upon the OPLS-AA force field with each parameter set as follows: method, LBFGRS; max no. of iterations, 10000; converge on, gradient; convergence threshold, 0.05.

Acknowledgment. We thank Miho Hosoi, Yoshiko Iwakura, Mie Tsuchida, Yasuyo Inagaki, and Yuuki Nawagawa for their technical support. We also thank Rie Ueda for the synthesis of NCL-2. This work was supported in part by JST PRESTO program (T.S.), Mitsubishi Chemical Corporation Fund (T.S.), Research Foundation for Electrotechnology of Chubu (T.S.), and a Grant-in-Aid for Scientific Research from the Japan Society for the Promotion of Science (N.M.).

Supporting Information Available: Purification of recombinant JMJD2C, JMJD2A, and glutathione-dependent FDH, and a detailed protocol of PHD inhibition assays. This material is available free of charge via the Internet at <http://pubs.acs.org>.

References

- (1) (a) Kubicek, S.; Jenuwein, T. A crack in histone lysine methylation. *Cell* **2004**, *119*, 903–906. (b) Bannister, A. J.; Kouzarides, T. Reversing histone methylation. *Nature* **2005**, *436*, 1103–1106. (c) Shi, Y. Histone lysine demethylases: emerging roles in development, physiology and disease. *Nat. Rev. Genet.* **2007**, *8*, 829–833.
- (2) (a) Shi, Y.; Lan, F.; Matson, C.; Mulligan, P.; Whetstine, J. R.; Cole, P. A.; Casero, R. A.; Shi, Y. Histone demethylation mediated by the nuclear amine oxidase homolog LSD1. *Cell* **2004**, *119*, 941–953. (b) Karytinov, A.; Fomeris, F.; Profumo, A.; Ciossani, G.; Battaglioli, E.; Binda, C.; Mattevi, A. A novel mammalian flavin-dependent histone demethylase. *J. Biol. Chem.* **2009**, *284*, 17775–17782.
- (3) Klose, R. J.; Kallin, E. M.; Zhang, Y. JmjC-domain-containing proteins and histone demethylation. *Nat. Rev. Genet.* **2006**, *7*, 715–727.
- (4) Cloos, P. A.; Christensen, J.; Agger, K.; Maiolica, A.; Rappsilber, J.; Antal, T.; Hansen, K. H.; Helin, K. The putative oncogene GASC1 demethylates tri- and dimethylated lysine 9 on histone H3. *Nature* **2006**, *442*, 307–311.
- (5) Ishimura, A.; Terashima, M.; Kimura, H.; Akagi, K.; Suzuki, Y.; Sugano, S.; Suzuki, T. Jmjd2c histone demethylase enhances the expression of Mdm2 oncogene. *Biochem. Biophys. Res. Commun.* **2009**, *389*, 366–371.
- (6) Wissmann, M.; Yin, N.; Müller, J. M.; Greschik, H.; Fodor, B. D.; Jenuwein, T.; Vogler, C.; Schneider, R.; Günther, T.; Buettner, R.; Metzger, E.; Schüle, R. Cooperative demethylation by JMJD2C and LSD1 promotes androgen receptor-dependent gene expression. *Nat. Cell Biol.* **2007**, *9*, 347–353.
- (7) Liu, G.; Bollig-Fischer, A.; Kreike, B.; van de Vijver, M. J.; Abrams, J.; Ethier, S. P.; Yang, Z. Q. Genomic amplification and oncogenic properties of the GASC1 histone demethylase gene in breast cancer. *Oncogene* **2009**, *28*, 4491–4500.
- (8) Smith, E. H.; Janknecht, R.; Maher, L. J., III. Succinate inhibition of alpha-ketoglutarate-dependent enzymes in a yeast model of paraganglioma. *Hum. Mol. Genet.* **2007**, *16*, 3136–3148.
- (9) Rose, N. R.; Ng, S. S.; Mecinovic, J.; Liénard, B. M. R.; Bello, S. H.; Sun, Z.; McDonough, M. A.; Oppermann, U.; Schofield, C. J. Inhibitor scaffolds for 2-oxoglutarate-dependent histone lysine demethylases. *J. Med. Chem.* **2008**, *51*, 7053–7056.
- (10) Hamada, S.; Kim, T. D.; Suzuki, T.; Itoh, Y.; Tsumoto, H.; Nakagawa, H.; Janknecht, R.; Miyata, N. Synthesis and activity of *N*-oxalylglycine and its derivatives as Jumonji C-domain-containing histone lysine demethylase inhibitors. *Bioorg. Med. Chem. Lett.* **2009**, *19*, 2852–2855.
- (11) Rose, N. R.; Woon, E. C. Y.; Kingham, G. L.; King, O. N. F.; Mecinović, J.; Clifton, I. J.; Ng, S. S.; Talib-Hardy, J.; Oppermann, U.; McDonough, M. A.; Schofield, C. J. Selective inhibitors of the JMJD2 histone demethylases: Combined nondenaturing mass spectrometric screening and crystallographic approaches. *J. Med. Chem.* **2010**, *53*, 1810–1818.
- (12) Sekirnik, R.; Rose, N. R.; Thalhammer, A.; Seden, P. T.; Mecinović, J.; Schofield, C. J. Inhibition of the histone lysine demethylase JMJD2A by ejection of structural Zn(II). *Chem. Commun.* **2009**, 6376–6378.
- (13) Ng, S. S.; Kavanagh, K. L.; McDonough, M. A.; Butler, D.; Pilka, E. S.; Liénard, B. M.; Bray, J. E.; Savitsky, P.; Gileadi, O.; von Delft, F.; Rose, N. R.; Offer, J.; Scheinost, J. C.; Borowski, T.; Sundstrom, M.; Schofield, C. J.; Oppermann, U. Crystal structures of histone demethylase JMJD2A reveal basis for substrate specificity. *Nature* **2007**, *448*, 87–91.
- (14) Cannizzaro, C. E.; Houk, K. N. Magnitudes and chemical consequences of $R_3N^+-C-H \cdots O=C$ hydrogen bonding. *J. Am. Chem. Soc.* **2002**, *124*, 7163–7169.
- (15) Chowdhury, R.; McDonough, M. A.; Mecinović, J.; Loenarz, C.; Flashman, E.; Hewitson, K. S.; Domene, C.; Schofield, C. J. Structural basis for binding of hypoxia-inducible factor to the oxygen-sensing prolyl hydroxylase. *Structure* **2009**, *17*, 981–989.
- (16) (a) Suzuki, T.; Nagano, Y.; Kouketsu, A.; Matsuura, A.; Maruyama, S.; Kuronaki, M.; Nakagawa, H.; Miyata, N. Novel inhibitors of human histone deacetylases: Design, synthesis, enzyme inhibition, and cancer cell growth inhibition of SAHA-based non-hydroxamates. *J. Med. Chem.* **2005**, *48*, 1019–1032. (b) Suzuki, T.; Hisakawa, S.; Itoh, Y.; Maruyama, S.; Kurotaki, M.; Nakagawa, H.; Miyata, N. Identification of a potent and stable antiproliferative agent by the prodrug formation of a thiolate histone deacetylase inhibitor. *Bioorg. Med. Chem. Lett.* **2007**, *17*, 1558–1561.
- (17) Ueda, R.; Suzuki, T.; Mino, K.; Tsumoto, H.; Nakagawa, H.; Hasegawa, M.; Sasaki, R.; Mizukami, T.; Miyata, N. Identification of cell-active lysine specific demethylase 1-selective inhibitors. *J. Am. Chem. Soc.* **2009**, *131*, 17536–17537.
- (18) Roy, T. W.; Bhagwat, A. S. Kinetic studies of *Escherichia coli* AlkB using a new fluorescence-based assay for DNA demethylation. *Nucleic Acids Res.* **2007**, *35*, e147.
- (19) Oehme, F.; Jonghaus, W.; Narouz-Ott, L.; Huetter, J.; Flamme, I. A nonradioactive 96-well plate assay for the detection of hypoxia-inducible factor prolyl hydroxylase activity. *Anal. Biochem.* **2004**, *330*, 74–80.